



HAL
open science

Nested polyhedra model of turbulence

Özgür D. Gürçan

► **To cite this version:**

Özgür D. Gürçan. Nested polyhedra model of turbulence. *Physical Review E*, 2017, 95 (6), pp.063102. 10.1103/PhysRevE.95.063102 . hal-01548206

HAL Id: hal-01548206

<https://hal.sorbonne-universite.fr/hal-01548206>

Submitted on 27 Jun 2017

HAL is a multi-disciplinary open access archive for the deposit and dissemination of scientific research documents, whether they are published or not. The documents may come from teaching and research institutions in France or abroad, or from public or private research centers.

L'archive ouverte pluridisciplinaire **HAL**, est destinée au dépôt et à la diffusion de documents scientifiques de niveau recherche, publiés ou non, émanant des établissements d'enseignement et de recherche français ou étrangers, des laboratoires publics ou privés.

Nested polyhedra model of turbulence

Ö. D. Gürçan*

*CNRS, Laboratoire de Physique des Plasmas, Ecole Polytechnique, 91120 Palaiseau,
and Sorbonne Universités, UPMC Université Paris 06, 75005 Paris, France*

(Received 10 March 2016; published 6 June 2017)

A discretization of the wave-number space is proposed, using nested polyhedra, in the form of alternating dodecahedra and icosahedra that are self-similarly scaled. This particular choice allows the possibility of forming triangles using only discretized wave vectors when the scaling between two consecutive dodecahedra is equal to the *golden ratio* and the icosahedron between the two dodecahedra is the dual of the inner dodecahedron. Alternatively, the same discretization can be described as a logarithmically spaced (with a scaling equal to the golden ratio), nested dodecahedron-icosahedron compounds. A wave vector which points from the origin to a vertex of such a mesh, can always find two other discretized wave vectors that are also on the vertices of the mesh (which is not true for an arbitrary mesh). Thus, the nested polyhedra grid can be thought of as a reduction (or decimation) of the Fourier space using a particular set of self-similar triads arranged approximately in a spherical form. For each vertex (i.e., discretized wave vector) in this space, there are either 9 or 15 pairs of vertices (i.e., wave vectors) with which the initial vertex can interact to form a triangle. This allows the reduction of the convolution integral in the Navier-Stokes equation to a sum over 9 or 15 interaction pairs, transforming the equation in Fourier space to a network of “interacting” nodes that can be constructed as a numerical model, which evolves each component of the velocity vector on each node of the network. This model gives the usual Kolmogorov spectrum of $k^{-5/3}$. Since the scaling is logarithmic, and the number of nodes for each scale is constant, a very large inertial range (i.e., a very high Reynolds number) with a much lower number of degrees of freedom can be considered. Incidentally, by assuming isotropy and a certain relation between the phases, the model can be used to systematically derive shell models.

DOI: [10.1103/PhysRevE.95.063102](https://doi.org/10.1103/PhysRevE.95.063102)

I. INTRODUCTION

Turbulence is a complex phenomenon involving chaotic behavior over a range of scales. Yet it has important underlying symmetries and regularities. Both its unpredictable nature and its regular hierarchical structure are a result of the form of the nonlinear interactions. Therefore, the study of turbulence is a study of the nonlinear interaction and a struggle to understand the hierarchical structure of the underlying symmetries it implies and their limitations [1].

While the simple picture of a turbulent cascade, introduced by Kolmogorov, involves interactions between different “scales” (i.e., wave-number magnitudes k) of a conserved quantity, the Navier-Stokes equation does not readily uphold this picture. One usually has to write the equation for a conserved quadratic quantity, such as the energy or kinetic helicity, and assume statistical isotropy, homogeneity, etc., in order to arrive at a description that is literally consistent with the basic cascade picture [2]. However, it is clear that the nonlinear cascade happens in the original equation, even without these assumptions. For instance, even without any assumption of isotropy, the energy is transferred from wave number to wave number. If one uses a representation of the wave vector in spherical polar coordinates in k space [i.e., using k, θ_k, ϕ_k , such that $(k_x, k_y, k_z) = (k \sin \theta_k \cos \phi_k, k \sin \theta_k \sin \phi_k, k \cos \theta_k)$], one can describe how the energy would be transferred from k to k' , which is closely related to what we call the “cascade”, even if the cascade, as such, is not the only thing that is implied by the nonlinear interaction.

It is therefore tempting to imagine a discretization of the k space using some form of spherical polar coordinates, which would assign the phenomenon of nonlinear cascade to a particular direction k . Furthermore, one may introduce a logarithmic discretization, so that with only a small number of points, one may cover a large range in this direction. In the study of weak wave turbulence, where the frequency and the wave number can be linked using a dispersion relation, such a logarithmic grid may be used without any difficulty (e.g., see Ref. [3] for weak magnetohydrodynamic turbulence). It is also commonly used in isotropic cascade modeling using closures, such as the eddy-damped quasilinear Markovian approximation [4–6] and differential approximation models [7–9]. Cascade models that use a logarithmic discretization, or shell models (see, for example, Ref. [10]), are also simplified models that try to exploit this particular aspect of the geometry of the turbulent cascade. Logarithmically discretized models for two-dimensional (2D) turbulence, which can be derived from a systematic self-similar reduction of the Fourier space [11], can also be counted among these models.

More generally, the reduction of a continuous, but self-similar system to a finite number of interacting modes [12], respecting the original self-similar structure, has been studied in the past for cascade models based on the structure of Burger’s equation [13] or the Navier-Stokes equation [14], especially in the context of earlier high-resolution simulation efforts [15]. Such reduction procedures have played an important role, beyond simple numerical convenience, in turbulence studies by providing theoretical insight into the underlying hierarchical structure of the dynamics of turbulence [16–18]. Since one of the primary goals of the study of turbulence is a reduction of the degrees of freedom in turbulent dynamics

*ozgur.gurcan@lpp.polytechnique.fr

as faithfully as possible to its essential features, such models were studied for various aspects. It was found, for instance, that severely reduced models, such as shell models, which rely on a truncation of the original system to keep only local interactions, recover both the wave-number spectrum and its intermittency [19–21]. However, how the shell model gets the intermittency correction is still controversial.

In the same spirit, here we present a direct discretization of the Navier-Stokes equation in \mathbf{k} space on a special mesh constructed from self-similarly scaled dodecahedron-icosahedron compounds (i.e., Wenninger model index 47 [22]). As shown below, choosing the scaling between two consecutive dodecahedron-icosahedron compounds equal to the *golden ratio* allows the possibility of forming triangles using only discretized wave vectors. The same grid can be obtained by considering nested, alternating icosahedra and dodecahedra where the scaling between the inner dodecahedron and the outer icosahedron is the square root of the golden ratio times the factor $\sqrt{\sqrt{5}/3}$ so that the two consecutive polyhedra are the duals of one another.

The model as introduced here may appear artificial, as it is composed of rather complicated-sounding polyhedra. However, it is a minimal model in the sense that the icosahedron is the minimal basis for the *icosphere*, which is an approximation to a sphere with a roughly equal vertex density everywhere on its surface (unlike a straightforward discretization of angles, which results in a higher vertex density near the poles), and that its dual polyhedron, the dodecahedron, is necessary for completing the triads formed by the position vectors (in k space) of its vertices.

The method of reduction, which could be generalized, can be thought of as a *discretization based on wave-vector triads* instead of a more classical discretization based on wave vectors themselves. Note that the imposed self-similar structure of the model enforces a uniform triad density as a function of the scale, which is known to be incorrect in the case of turbulence and appears to be an important weakness of the model. However, the model gives the correct wave-number spectrum and it can describe anisotropy in three dimensions. Furthermore, a higher-order method, based on algorithmic construction of the grid, may be imagined where wave vectors picked from two distant (i.e., nonconsecutive) polyhedra could be used to deduce a third polyhedron by completing the triads.

It can be speculated that such a structure may be meaningful beyond the model itself as a crystalline state in wave-number space, which could be tailored by choosing the initial conditions and the driving to fall on the vertices of a compound polyhedron, and the vertices of such an object would interact with each other to drive other objects that are self-similar scalings of the initial object as well as other higher-order compound objects.

II. THE NESTED POLYHEDRA MODEL

Consider the Navier-Stokes equation in Fourier space:

$$\partial_t u_{\mathbf{k}}^i + i k_{\kappa} \left[\delta_{ij} - \frac{k_i k_j}{k^2} \right] \sum_{\mathbf{p}+\mathbf{q}=-\mathbf{k}} u_{\mathbf{p}}^{\kappa*} u_{\mathbf{q}}^j = 0. \quad (1)$$

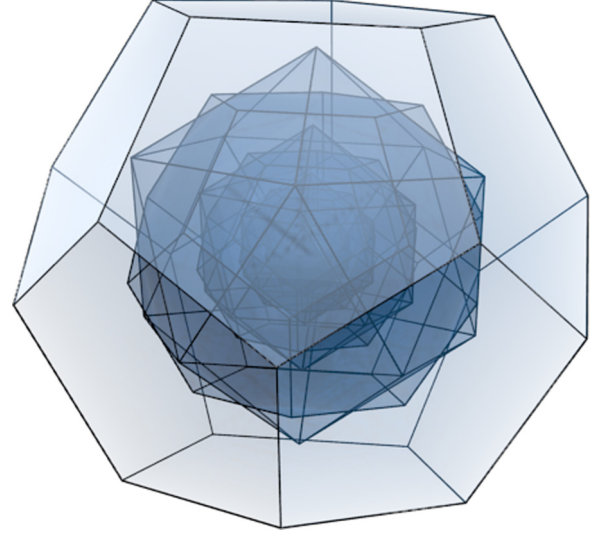


FIG. 1. Alternating dodecahedron-icosahedron shells covering the Fourier space. Each \mathbf{k} starts at the origin and ends at one of the vertices of this object.

We propose a discretization of the k space using a logarithmic alternating icosahedral-dodecahedral basis (see Fig. 1),

$$\mathbf{k} = k_n \hat{\mathbf{k}}_{\ell},$$

where $k_n = g^n \lambda k_0$ is the logarithmically spaced wave-number magnitude with $g = \sqrt{(1 + \sqrt{5})/2}$,

$$\lambda = \begin{cases} \sqrt{\frac{\sqrt{5}}{3}} & \text{for icosahedron,} \\ 1 & \text{for dodecahedron,} \end{cases}$$

and

$$\hat{\mathbf{k}}_{\ell} = e_{\ell}^j = [\sin \theta_{\ell} \cos \phi_{\ell}, \sin \theta_{\ell} \sin \phi_{\ell}, \cos \theta_{\ell}], \quad (2)$$

where θ_{ℓ} and ϕ_{ℓ} are to be picked from the angles corresponding to the icosahedral and the dodecahedral vertices, listed in Table I. It is shown below that this choice comes from the

TABLE I. Polar and azimuthal angles θ and ϕ of a dodecahedron and an icosahedron. Here $\alpha = \arcsin(\varphi/\sqrt{3}) - \arccos(\varphi/\sqrt{\varphi+2})$, $\beta = \arctan(2\varphi^2)$, and $\gamma = \pi/2 - \arctan(1/2)$ with $\varphi = (1 + \sqrt{5})/2$.

Dodecahedron						Icosahedron		
ℓ	θ_{ℓ}	ϕ_{ℓ}	ℓ	θ_{ℓ}	ϕ_{ℓ}	ℓ	θ_{ℓ}	ϕ_{ℓ}
0	α	$\pi/5$	10	$\pi - \alpha$	$6\pi/5$	0	0	.
1	α	$3\pi/5$	11	$\pi - \alpha$	$8\pi/5$	1	γ	0
2	α	π	12	$\pi - \alpha$	0	2	γ	$2\pi/5$
3	α	$7\pi/5$	13	$\pi - \alpha$	$2\pi/5$	3	γ	$4\pi/5$
4	α	$9\pi/5$	14	$\pi - \alpha$	$4\pi/5$	4	γ	$6\pi/5$
5	β	$\pi/5$	15	$\pi - \beta$	$6\pi/5$	5	γ	$8\pi/5$
6	β	$3\pi/5$	16	$\pi - \beta$	$8\pi/5$	6	π	.
7	β	π	17	$\pi - \beta$	0	7	$\pi - \gamma$	π
8	β	$7\pi/5$	18	$\pi - \beta$	$2\pi/5$	8	$\pi - \gamma$	$7\pi/5$
9	β	$9\pi/5$	19	$\pi - \beta$	$4\pi/5$	9	$\pi - \gamma$	$9\pi/5$
						10	$\pi - \gamma$	$\pi/5$
						11	$\pi - \gamma$	$3\pi/5$

condition of forming triads with the vertices of the three consecutive polyhedra.

Note that by enumerating the vertices of the icosahedron and the dodecahedron, we reduce the number of indices necessary to describe a given wave vector from three to two (i.e., using only n and ℓ , we can define a unique wave vector). It is also important to mention that since the original velocity field $\mathbf{u}(\mathbf{x}, t)$ is real, its Fourier transform has the symmetry that $\mathbf{u}(\mathbf{k}, t) = \mathbf{u}^*(-\mathbf{k}, t)$. The assignments of numbers to vertices are made such that $\hat{\mathbf{k}}_{\ell+N_\ell/2} = -\hat{\mathbf{k}}_\ell$, where N_ℓ is the number of vertices of the polyhedron under consideration (i.e., $N_\ell = 12$ for the icosahedron, $N_\ell = 20$ for the dodecahedron). This symmetry can be used to reduce the number of degrees of freedom by half. Otherwise, one must be careful that the initial conditions as well as all the terms in the equation (such as forcing, dissipation, etc.) respect this symmetry.

Three-dimensional turbulence requires solving three vector components of the velocity. Here we use Cartesian coordinates $\mathbf{u}_{\mathbf{k}} = u_{k_n \hat{\mathbf{k}}_i}^{(x)} \hat{\mathbf{x}} + u_{k_n \hat{\mathbf{k}}_i}^{(y)} \hat{\mathbf{y}} + u_{k_n \hat{\mathbf{k}}_i}^{(z)} \hat{\mathbf{z}} \rightarrow u_{n\ell}^i \hat{\mathbf{x}}_i$. In this representation, the Navier-Stokes equation becomes

$$\partial_t u_{n,\ell}^i + i k_{n\ell}^\kappa \left[\delta_{ij} - \frac{k_{n\ell}^i k_{n\ell}^j}{k_n^2} \right] \sum_{n',\ell'} u_{n'\ell'}^{i*} u_{n''\ell''}^{j*} = 0, \quad (3)$$

where ℓ'' and n'' can be inferred from n , ℓ , n' , and ℓ' using the fact that the corresponding wave numbers form a triad,

$$k_n \hat{\mathbf{k}}_\ell + k_{n'} \hat{\mathbf{k}}_{\ell'} + k_{n''} \hat{\mathbf{k}}_{\ell''} = 0,$$

consider three consecutive spherical shells such that $n' = n - 1$ and $n'' = n + 1$, and take alternating spheres to be discretized as dodecahedrons and icosahedrons (i.e., $n = 1$ is an icosahedron, $n = 2$ is a dodecahedron, $n = 3$ is an icosahedron, and so on), we can write

$$k_n \hat{\mathbf{k}}_\ell^i + k_{n-1} \hat{\mathbf{k}}_{\ell'}^d + k_{n+1} \hat{\mathbf{k}}_{\ell''}^d = 0, \quad (4)$$

$$k_n \hat{\mathbf{k}}_\ell^d + k_{n-1} \hat{\mathbf{k}}_{\ell'}^i + k_{n+1} \hat{\mathbf{k}}_{\ell''}^i = 0, \quad (5)$$

which can be shifted in n (i.e., $n \rightarrow n + 1$ and $n \rightarrow n - 1$) to cover all the necessary triads. Note that other interactions do not correspond to grid points and are dropped. It is interesting to note that this does not lead to leaking of conserved quantities.

Now consider $\ell = 0$, $\ell' = 5$, $\ell'' = 10$ for the first equation:

$$\begin{aligned} & \left[g \sin(\pi - \alpha) \cos \frac{6\pi}{5} + g^{-1} \sin \beta \cos \frac{\pi}{5} \right] \hat{\mathbf{x}} \\ & + \left[g \sin(\pi - \alpha) \sin \frac{6\pi}{5} + g^{-1} \sin \beta \sin \frac{\pi}{5} \right] \hat{\mathbf{y}} \\ & + [\lambda + g^{-1} \cos \beta + g \cos(\pi - \alpha)] \hat{\mathbf{z}} = 0. \end{aligned}$$

Here the coefficients of $\hat{\mathbf{x}}$ and $\hat{\mathbf{y}}$ can be made to vanish by choosing $g = \sqrt{\varphi} = \sqrt{(1 + \sqrt{5})/2}$, while in order to make the coefficient of $\hat{\mathbf{z}}$ vanish, we need to choose the scaling of the radius of the icosahedron with respect to $g'' k_0$ as $\lambda = \sqrt{\frac{\sqrt{5}}{3}}$. This way we can satisfy the condition of the triad. The icosahedron that is constructed in this way is actually nothing but the dual icosahedron of the inner dodecahedron with radius k_{n-1} . While these two can be thought of as being on separate

TABLE II. Two dodecahedral vertices from neighboring shells (i.e., $n - 1$ and $n + 1$) that form a perfect triad with the icosahedral vertex at shell n .

$\ell_i:(n)$	$\ell'_d:(n-1)$	$\ell''_d:(n+1)$	$\ell_i:(n)$	$\ell'_d:(n-1)$	$\ell''_d:(n+1)$
0	5	10	3	0	11
	6	11		18	16
	7	12		14	9
	8	13		15	17
	9	14		3	12
1	1	10	4	1	12
	18	15		19	17
	12	7		10	5
	16	19		16	18
	3	14		4	13
2	4	10	5	2	13
	17	15		15	18
	13	8		11	6
	19	16		17	19
	2	11		0	14

shells in k space, since their radii are different, they could also be thought as sampling a single shell together in the form of a dodecahedron-icosahedron compound (the shell boundary in this case could be thought to be between the two consecutive compounds).

Of course one can rotate the triangle around the primary vector \mathbf{k} to obtain another interacting pair. For instance, for the node $\ell = 0$, the condition of the triad will be satisfied by the pairs $\{\ell', \ell''\} = [\{5, 10\}, \{6, 11\}, \{7, 12\}, \{8, 13\}, \{9, 14\}]$. Since each vertex of the icosahedron is equivalent, we can compute the interacting pairs of dodecahedral vertices for each vertex of the icosahedron using the same algorithm. The node-pair connections obtained in this way are listed in Tables II and III.

TABLE III. Two icosahedral vertices from neighboring shells (i.e., $n - 1$ and $n + 1$) that form a perfect triad with the dodecahedral vertex at shell n .

$\ell_d:(n)$	$\ell'_i:(n-1)$	$\ell''_i:(n+1)$	$\ell_d:(n)$	$\ell'_i:(n-1)$	$\ell''_i:(n+1)$
0	4	6	5	3	8
	9	7		5	7
	11	8		6	4
1	5	6	6	1	8
	7	9		4	9
	10	8		6	5
2	1	6	7	2	9
	11	9		5	10
	8	10		6	1
3	2	6	8	3	10
	9	11		1	11
	7	10		6	2
4	3	6	9	2	7
	8	11		4	11
	10	7		6	3

Now consider (5), and choose $\ell = 0$, $\ell' = 6$, $\ell'' = 4$. This gives

$$\begin{aligned} & \left(\sin \alpha \cos \frac{\pi}{5} + g^{-1} \lambda \sin \gamma \cos \frac{6\pi}{5} \right) \hat{\mathbf{x}} \\ & + \left(\sin \alpha \sin \frac{\pi}{5} + g^{-1} \lambda \sin \gamma \sin \frac{6\pi}{5} \right) \hat{\mathbf{y}} \\ & + \left(\cos \alpha + g^{-1} \lambda \cos \gamma - \lambda g \right) \hat{\mathbf{z}} = 0, \end{aligned}$$

which is automatically satisfied by the earlier choices $g = \sqrt{\varphi}$ and $\lambda = \sqrt{\sqrt{5}/3}$. Note again that the above condition for $\ell = 0$ is also satisfied by the pairs $\{\ell', \ell''\} = [\{4, 6\}, \{9, 7\}, \{11, 8\}]$. Similarly to the case where the icosahedron was in the middle, we can find the rest of the interacting pairs of icosahedral vertices for each vertex of the dodecahedron by rotating the mesh.

Since by exchanging $(n', \ell') \leftrightarrow (n'', \ell'')$ we obtain another interaction, we consider this explicitly by symmetrizing the equations as

$$\partial_t u_{n\ell}^i + i M_{n\ell}^{\kappa ij} \sum_{n' < n'', \ell'} (u_{n'\ell'}^{\kappa*} u_{n''\ell''}^{j*} + u_{n''\ell''}^{\kappa*} u_{n'\ell'}^{j*}) = 0, \quad (6)$$

where

$$M_{n\ell}^{\kappa ij} = k_{n\ell}^{\kappa} \left[\delta_{ij} - \frac{k_{n\ell}^i k_{n\ell}^j}{k_{n\ell}^2} \right].$$

In this way we can go over each node-pair connection once, without paying attention to the sign, and all possible interactions will be covered. Defining n as the flattened node number (e.g., $\{n, \ell\} = \{3, 3\} \rightarrow n = 12 \times 2 + 20 + 3 = 47$ if the first shell is an icosahedron), instead of the shell number as before,

$$\partial_t u_n^i + i M_n^{\kappa ij} \sum_{\{n', n''\} = \mathbf{p}_n} (u_{n'}^{\kappa*} u_{n''}^{j*} + u_{n''}^{\kappa*} u_{n'}^{j*}) = 0, \quad (7)$$

where the sum is computed over the interacting $\{n', n''\}$ pairs of a node n (e.g., \mathbf{p}_{47} is the list of the pairs of nodes shown in Fig. 2). These connections can be obtained using Tables II and III and the flattening rule $m = \text{floor}(n/2) \times 32 + (n \bmod 2) \times N_{fs} + \ell$ (and then $m \rightarrow n$), where N_{fs} is the number of vertices of the first shell, and can be thought of as a regular network model (see Fig. 2). The set of triangles that are involved in the interactions of three consecutive polyhedra are shown in Figs. 3 and 4 where some triads are arbitrarily highlighted for easier distinction. Note that in (7) the interaction matrix $M_{n\ell}^{\kappa ij} \rightarrow M_n^{\kappa ij}$ is also flattened in the same way as the vector $u_{n\ell}^i \rightarrow u_n^i$.

A. Further simplifications

As discussed earlier, in order to reduce the degrees of freedom of the nested polyhedra model of turbulence, one may consider only half of each polyhedron (for instance, the $k_z > 0$ hemisphere) and obtain the other half using the relation $\mathbf{u}_{-\mathbf{k}} = \mathbf{u}_{\mathbf{k}}^*$. In order to achieve this, in practice one has to keep in mind whether or not a node in an interaction is conjugated [i.e., in Tables II and III if the node number falls into the upper hemisphere it will be conjugated, and if it falls into the lower hemisphere it will not be conjugated, in

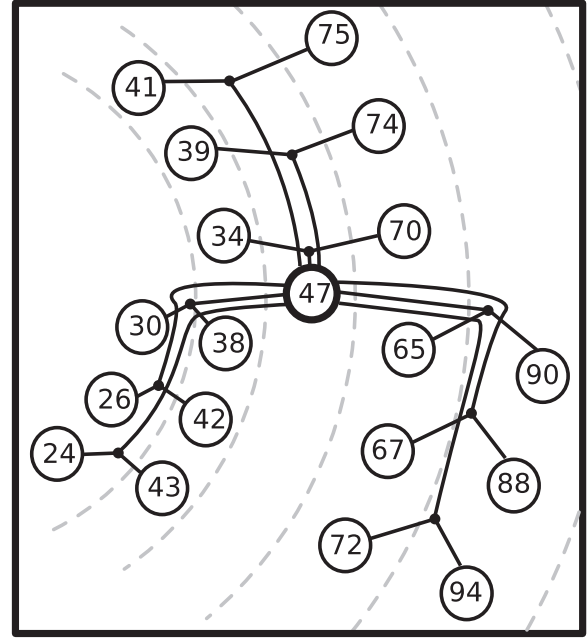


FIG. 2. Pairs of nodes interacting with node number 47 (i.e., node $\ell = 3$ on shell $n = 3$), where the first shell is an icosahedron, which is shown here as an example.

Eq. (7)]. This can be done by keeping a “conjugated flag” for each interaction between nodes. In addition to decreasing the number of degrees of freedom by half, this approach has the advantage of automatically imposing the reality condition of the velocity field as a function of space, which is important and is not exact in the more straightforward formulation.

Another, more interesting simplification is to consider the helical decomposition, which allows the reduction of the velocity 3-vector to two scalars, representing right-handed and left-handed helicities with respect to the wave number. This is possible because of the fact that the velocity field is divergence-free in the Navier-Stokes equation, and therefore its projection onto the wave number has to vanish. This formulation allows

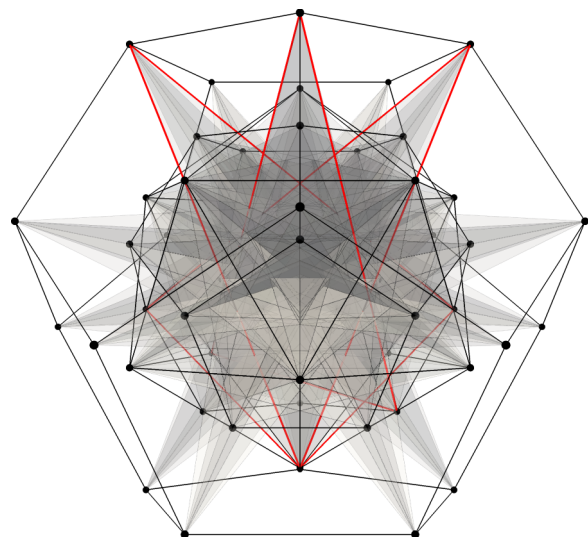


FIG. 3. All the k -space triads corresponding to an icosahedron squeezed in between two dodecahedra.

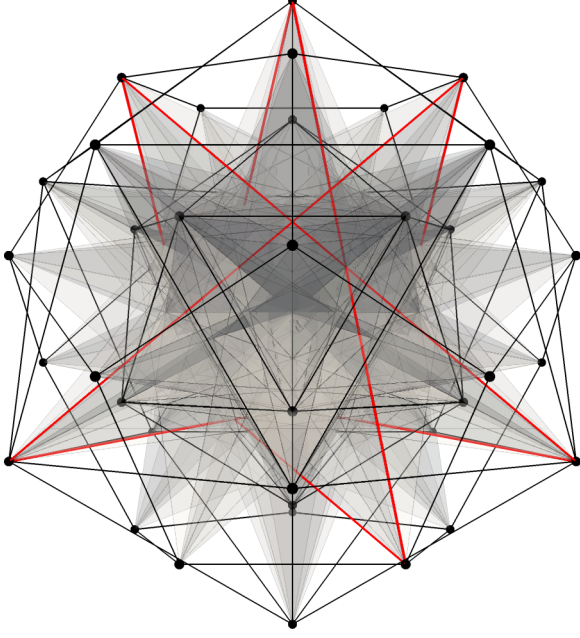


FIG. 4. All the k -space triads corresponding to a dodecahedron squeezed between two icosahedra.

us to reduce the number of degrees of freedom to $2/3$ times the initial number and it guarantees that the velocity field remains divergence-free, in contrast to the straightforward method, which does not guarantee this numerically.

Together these two simplifications would permit a reduction of the number of degrees of freedom to $1/3$ times the initial number and guarantee a real and divergence-free velocity field as a function of space.

Note that a simple spherical representation of the velocity field in \mathbf{k} space (i.e., $\mathbf{u}_{n\ell} = u_{n\ell}^k \hat{\mathbf{k}}_{n\ell} + u_{n\ell}^\theta \hat{\boldsymbol{\theta}}_{n\ell} + u_{n\ell}^\phi \hat{\boldsymbol{\phi}}_{n\ell}$) also reduces the velocity field to two dimensions since the ‘‘radial’’ component vanishes (i.e., $u_{n\ell}^k = \mathbf{u}_{n\ell} \cdot \hat{\mathbf{k}}_{n\ell} = 0$). However, the simplification of the interaction coefficients as well as the direct physical interpretation in terms of helicity is lost in this representation. Nonetheless, this representation allows us to see that the Fourier-transformed velocity field is everywhere tangential to the spherical shells in k space.

Further reduction can be achieved by associating one kind of helicity (i.e., right) with one type of polyhedron (i.e., dodecahedron) and the other kind of helicity (i.e., left) with the other type of polyhedron (i.e., icosahedron). This reduces the number of degrees of freedom further by half. It also assigns a physical sense to the different types of polyhedra in the model. The reduced model obtained in this way can be written as

$$\partial_t u_{n\ell}^{s_n} + \frac{1}{4} \sum_{n' < n'', \ell'} (k_{n'} s_{n'} - k_{n''} s_{n''}) \times (\hat{\mathbf{h}}_\ell^{s_n*} \cdot \hat{\mathbf{h}}_{\ell'}^{s_{n'}*} \times \hat{\mathbf{h}}_{\ell''}^{s_{n''}*}) u_{n'\ell'}^{s_{n'}*} u_{n''\ell''}^{s_{n''}*} = -\nu k_n^2 u_{n,\ell}^{s_n},$$

where

$$\mathbf{u}(\mathbf{x}) = \sum_{n=0}^N u_{n\ell}^{s_n} \hat{\mathbf{h}}_\ell^{s_n} \quad (8)$$

and $s_n = (+)$ if n :even, and $s_n = (-)$ if n :odd, with

$$\hat{\mathbf{h}}_{n\ell}^\pm = \hat{\mathbf{v}}_{\mathbf{k}} \times \hat{\mathbf{k}} \pm i \hat{\mathbf{v}}_{\mathbf{k}},$$

$$\hat{\mathbf{v}}_{\mathbf{k}} = \frac{\mathbf{k} \times \hat{\mathbf{z}}}{|\mathbf{k} \times \hat{\mathbf{z}}|}.$$

This gives

$$\begin{aligned} \partial_t u_{n,\ell}^{(+)} + k_n g^{-2} (1 + \lambda g) \sum_{\{\ell', \ell''\}} (\hat{\mathbf{h}}_\ell^{(+)*} \cdot \hat{\mathbf{h}}_{\ell'}^{(+)*} \times \hat{\mathbf{h}}_{\ell''}^{(-)*}) u_{n-2,\ell'}^{(+)*} u_{n-1,\ell''}^{(-)*} \\ - \lambda k_n g^{-1} (g^2 - 1) \sum_{\{\ell', \ell''\}} (\hat{\mathbf{h}}_\ell^{(+)*} \cdot \hat{\mathbf{h}}_{\ell'}^{(-)*} \times \hat{\mathbf{h}}_{\ell''}^{(-)*}) u_{n-1,\ell'}^{(-)*} u_{n+1,\ell''}^{(-)*} \\ - k_n g (\lambda + g) \sum_{\{\ell', \ell''\}} (\hat{\mathbf{h}}_\ell^{(+)*} \cdot \hat{\mathbf{h}}_{\ell'}^{(-)*} \times \hat{\mathbf{h}}_{\ell''}^{(+)*}) u_{n+1,\ell'}^{(-)*} u_{n+2,\ell''}^{(+)*} \\ = -\nu k_n^2 a_{n,\ell}^{(+)} \end{aligned}$$

for even n and

$$\begin{aligned} \partial_t u_{n,\ell}^{(-)} - k_n g^{-2} (\lambda + g) \sum_{\{\ell', \ell''\}} (\hat{\mathbf{h}}_\ell^{(-)*} \cdot \hat{\mathbf{h}}_{\ell'}^{(-)*} \times \hat{\mathbf{h}}_{\ell''}^{(+)*}) u_{n-2,\ell'}^{(-)*} u_{n-1,\ell''}^{(+)*} \\ + k_n g^{-1} (1 - g^2) \sum_{\{\ell', \ell''\}} (\hat{\mathbf{h}}_\ell^{(-)*} \cdot \hat{\mathbf{h}}_{\ell'}^{(+)*} \times \hat{\mathbf{h}}_{\ell''}^{(+)*}) u_{n-1,\ell'}^{(+)*} u_{n+1,\ell''}^{(+)*} \\ + k_n g (1 + \lambda g) \sum_{\{\ell', \ell''\}} (\hat{\mathbf{h}}_\ell^{(-)*} \cdot \hat{\mathbf{h}}_{\ell'}^{(+)*} \times \hat{\mathbf{h}}_{\ell''}^{(-)*}) u_{n+1,\ell'}^{(+)*} u_{n+2,\ell''}^{(-)*} \\ = -\nu k_n^2 u_{n,\ell}^{(-)} \end{aligned}$$

for odd n .

It is interesting to note that these two equations have the same form (apart from the additional ℓ resolution) as the model discussed in Ref. [23]. In particular, the above form corresponds to the model SM1 as discussed in that paper.

B. Conservation laws

Energy conservation can be shown by considering the energy of a single triad (e.g., $\mathbf{k}_{n\ell}$, $\mathbf{k}_{n-1,\ell'}$, and $\mathbf{k}_{n+1,\ell''}$),

$$\begin{aligned} \frac{dE_\Delta}{dt} = \text{Re} [i \overline{M}_{n\ell}^{\kappa ij} u_{n-1,\ell'}^{\kappa*} u_{n+1,\ell''}^{j*} u_{n\ell}^{i*} \\ + i \overline{M}_{n-1,\ell'}^{\kappa ij} u_{n-1,\ell'}^{i*} u_{n,\ell}^{\kappa*} u_{n+1,\ell''}^{j*} \\ + i \overline{M}_{n+1,\ell''}^{\kappa ij} u_{n+1,\ell''}^{i*} u_{n-1,\ell'}^{\kappa*} u_{n\ell}^{j*}] = 0, \end{aligned}$$

by using the form of $\overline{M}_{n\ell}^{\kappa ij}$ and the facts that $k_{n\ell}^i u_{n\ell}^i = 0$ and $k_{n\ell}^i = -k_{n-1,\ell'}^i - k_{n+1,\ell''}^i$. The total energy can then be written as the sum of the energy E_Δ over triads. Since each closed triad conserves energy, any discretization of the Fourier space using a reduced set of ‘‘triads’’ automatically respects energy conservation. In fact this should be true for all the conservation laws of the system even without explicit knowledge of the conservation laws. This is important, as we see later, since it provides a ‘‘derivation’’ of shell models and their generalizations without detailed knowledge of the conservation laws. A similar effort was discussed earlier for 2D turbulence [11].

C. Connection to shell models

When the sum over different n values is written explicitly, the model takes the form

$$\partial_t u_{n,\ell}^i + i \overline{M}_{n\ell}^{kij} \sum_{\{\ell', \ell''\}} [u_{n-2,\ell'}^{k*} u_{n-1,\ell''}^{j*} + u_{n-1,\ell'}^{k*} u_{n+1,\ell''}^{j*} + u_{n+1,\ell'}^{k*} u_{n+2,\ell''}^{j*}] \quad (9)$$

regardless of whether the n th shell is an icosahedron or a dodecahedron. Note that $\overline{M}_{n\ell}^{kij} = M_{n\ell}^{kij} + M_{n\ell}^{jik}$ and the sum is computed over pairs of interacting nodes of the consecutive shells as listed in Tables II and III. The basic form of Eq. (9) is consistent with the Gledzer-Ohkitani-Yamada (GOY) model [19]. In fact one can arrive at a form very similar to the GOY model by arranging a certain (rather particular) choice of phases and signs of helicities for each node. Taking

$$u_{n,\ell}^j = u_n e^{i\theta_{n,\ell}^j}$$

and imposing the resulting coefficients to be independent of ℓ (see below for a discussion of this), we get

$$\partial_t u_n + ik_n (a_n u_{n-2}^* u_{n-1}^* + b_n u_{n-1}^* u_{n+1}^* + c_n u_{n+1}^* u_{n+2}^*), \quad (10)$$

where

$$\begin{aligned} a_n &\equiv \sum_{\{\ell', \ell''\}} \hat{\mathbf{k}}_{n\ell}^j (\delta_{ik} - \hat{\mathbf{k}}_{n\ell}^k \hat{\mathbf{k}}_{n\ell}^i) [e^{-i\xi_{n,\ell',\ell''}^{kji}} + e^{-i\xi_{n,\ell',\ell''}^{jki}}], \\ b_n &\equiv \sum_{\{\ell', \ell''\}} \hat{\mathbf{k}}_{n\ell}^j (\delta_{ik} - \hat{\mathbf{k}}_{n+1,\ell'}^k \hat{\mathbf{k}}_{n\ell}^i) [e^{-i\xi_{n+1,\ell',\ell''}^{kij}} + e^{-i\xi_{n+1,\ell',\ell''}^{jik}}], \\ c_n &\equiv \sum_{\{\ell', \ell''\}} \hat{\mathbf{k}}_{n\ell}^j (\delta_{ik} - \hat{\mathbf{k}}_{n\ell}^k \hat{\mathbf{k}}_{n\ell}^i) [e^{-i\xi_{n+2,\ell',\ell''}^{kij}} + e^{-i\xi_{n+2,\ell',\ell''}^{jik}}], \end{aligned}$$

and

$$\xi_{n,\ell',\ell''}^{kji} \equiv \theta_{n-2,\ell'}^k + \theta_{n-1,\ell''}^j + \theta_{n,\ell}^i.$$

The fact that (10) loses its dependence on ℓ (as the system is summed over ℓ' and ℓ'') means that the a_n , b_n , and c_n as defined above should be identical for all ℓ values of a polyhedron.

Assuming that the phases repeat after each four shells (i.e., $\theta_{n+4,\ell}^i = \theta_{n,\ell}^i$) gives $(6 + 10) \times 2 = 32$ independent nodes, and having two independent vector components for velocity each, we have 64 independent phases. The idea that the coefficients of (10) be independent of ℓ can be written as

$$a_{n\ell} = a_n, \quad b_{n\ell} = b_n, \quad c_{n\ell} = c_n$$

for any ℓ . In total this would give $3 \times 32 = 96$ equations. (Here 3 is the number of coefficients per node and 32 is the number of nodes. Note that the number of components does not enter, since the coefficients $a_{n\ell}$, $b_{n\ell}$, and $c_{n\ell}$ are already summed over i , j , and κ). However, the equations for $c_{n+2,\ell}$, $c_{n+3,\ell}$, and $b_{n+3,\ell}$ involve the phases $\xi_{n+4,\ell,\ell',\ell''}$, $\xi_{n+5,\ell',\ell,\ell''}$, and $\xi_{n+4,\ell,\ell',\ell''}$, which are the same as $\xi_{n,\ell,\ell',\ell''}$, $\xi_{n+1,\ell',\ell,\ell''}$, and $\xi_{n,\ell,\ell',\ell''}$, respectively (due to the assumption of fourfold periodicity), resulting in some of the same equations as before. If we assume that the n th shell is an icosahedron, the number of repeated equations is $(2 \times 10 + 1 \times 6) \times 2 = 52$, which reduces the number of independent equations to 44.

If the n th shell is a dodecahedron, on the other hand, the number of repeated equations is $(2 \times 6 + 1 \times 10) \times 2 = 44$, which results in 52 independent equations. This means that we can actually pick the 64 independent phases in such a way that the 44 or 52 independent equations that guarantee a GOY-like model are satisfied, and we would still have 20 or 12 undetermined phases, which could be taken, for example, as the phases of the independent components of the $(n + 1)$ st polyhedron (i.e., $\theta_{n+1,\ell}^i$).

Note that this analytical exercise should qualify as an actual, rigorous derivation of the GOY model, starting from the nested polyhedra model, assuming isotropy, and imposing some particular phase relations. Since the nested polyhedra model comes from a systematic reduction of the triads in a self-similar way, the derivation provides a rigorous path from the initial field equations to the shell model. Of course both the coefficients and the shell spacing are not free parameters, as they are imposed by the constraints of self-similarity of the nested polyhedra model.

D. Velocity field as a function of space

The 3D velocity field in real space implied by a k -space discretization using a set of vertices,

$$\mathbf{u}(\mathbf{x}) = \sum_n u_n^i e^{i\mathbf{k}_n \cdot \mathbf{x}} \hat{\mathbf{x}}_i \quad (11)$$

where $\hat{\mathbf{x}}_i$ is the unit vector in the i th direction (typically the x , y , and z directions). Now if we consider a single unit icosahedron (i.e., of radius $k_n = 1$), we can write the velocity field as

$$\begin{aligned} \mathbf{u}_{ico}(\mathbf{x}) &= \sum_{\ell=1}^6 (u_\ell^i e^{i\mathbf{k}_{n\ell} \cdot \mathbf{x}} + \text{c.c.}) \hat{\mathbf{x}}_i \\ &= \sum_{\ell=1}^6 (u_\ell^+ e^{i\mathbf{k}_{\ell} \cdot \mathbf{x}} \hat{\mathbf{h}}_\ell^+ + u_\ell^- e^{i\mathbf{k}_{\ell} \cdot \mathbf{x}} \hat{\mathbf{h}}_\ell^- + \text{c.c.}), \quad (12) \end{aligned}$$

which is defined by the 12 complex coefficients u_ℓ^\pm . These coefficients correspond to the weights of right- and left-handed helicities in six different directions that are defined by the icosahedron. The same can be done for a unit dodecahedron:

$$\mathbf{u}_{dod}(\mathbf{x}) = \sum_{\ell=1}^{10} (u_\ell^+ e^{i\mathbf{k}_{\ell} \cdot \mathbf{x}} \hat{\mathbf{h}}_\ell^+ + u_\ell^- e^{i\mathbf{k}_{\ell} \cdot \mathbf{x}} \hat{\mathbf{h}}_\ell^- + \text{c.c.}). \quad (13)$$

In order to see the real space structure of such a flow, we have considered an icosahedron-dodecahedron compound with randomly picked values for the coefficients u_ℓ^\pm , constructed the flow using (12) and (13), and plotted the result in Fig. 5.

E. Transition to two dimensions

There are various limiting cases, such as rotating turbulence, magnetohydrodynamic turbulence with a strong mean magnetic field, and turbulence in a thin film, where the turbulent dynamics become two-dimensional. However, there are some peculiar aspects of 2D turbulence and other peculiar aspects of 2D shell models (or logarithmically discretized models). Two-dimensional turbulence is generally believed to result in a dual cascade, where the enstrophy cascades in the forward and the energy cascades in the backward directions.

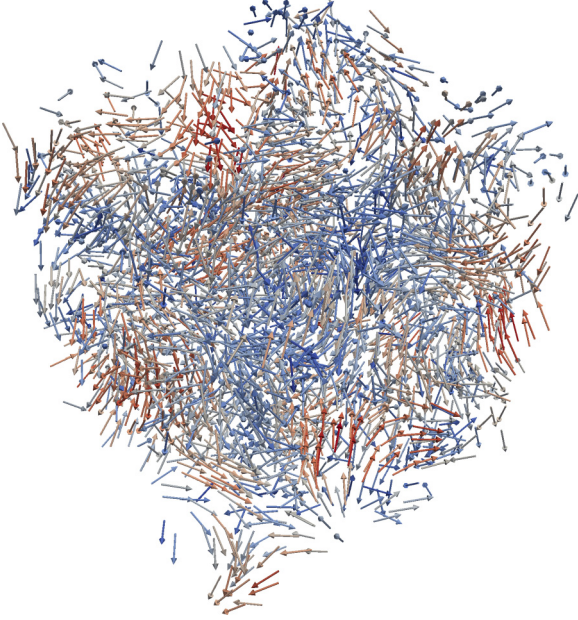


FIG. 5. The 3D velocity field corresponding to a single icosahedron-dodecahedron compound in Fourier space, with random phases for the Fourier coefficients.

However, logarithmic discretization of 2D space leads to the numerical inconvenience that the equipartition of energy between shells dominates over the inverse energy cascade. Thus, 2D shell models cannot describe the inverse energy cascade (unless there are additional terms in the equation, which keeps the system away from this tendency to equipartition). Interestingly, this is less of an issue in three-dimensional models. When the model is isotropic, however, it is impossible to study the transition from 3D to 2D, since all the directions are, by construction, the same. However, a nested polyhedra model can in principle be scaled in one direction (say the k_z direction), spherical shells can be flattened to pancakelike forms, and therefore the transition to 2D can be studied.

The limiting form of 2D turbulence can be obtained by simply setting $k_z = 0$ in the nested polyhedra structure of the grid. However, an interesting phenomenon takes place in this limit. The projection of nodes 1 to 5 of the n th icosahedron (which gives a regular pentagon) is the same as that of nodes 10 to 14 of the $(n+1)$ th and 15 to 19 of the $(n-1)$ th dodecahedra. Similarly, nodes 7 to 11 of the n th icosahedron are the same as nodes 0 to 4 of the $(n+1)$ th and 5 to 9 of the $(n-1)$ th dodecahedra. This means that the n th “shell” (really a circular ring or annulus) in a 2D model corresponds to at least three “shells”, n , $n+1$, and $n-1$, in a 3D model, as they fall exactly on the same points in the 2D space and they are indistinguishable and lead to degeneracy.

Note that $\alpha = \arcsin(\frac{2}{3\lambda g})$ is equivalent to the form listed in Table I for α . The smaller pentagon, which results from the projection of the inner points of a dodecahedron on the $k_z = 0$ plane, has a circumscribed circle of radius

$$k_{\perp} = \frac{2k}{3\lambda g}.$$

The larger pentagon, which comes from the projection of the outer points of the dodecahedron, and that which comes from those of its dual icosahedron have a circumscribed circle of radius

$$k_{\perp} = \frac{2gk}{3\lambda}.$$

This gives a scaling factor of g^2 between two consecutive circles. In other words, the wave numbers of the shells can now be defined with

$$k_{n\perp} = k_{0\perp}\varphi^n,$$

where $\varphi = g^2 = (1 + \sqrt{5})/2$ and $k_{0\perp} = \frac{2k_0}{3\lambda g} = \frac{2\sqrt{2}}{\sqrt{3(5+\sqrt{5})}}k_0$.

The equations for the shells can be obtained by projection also. The helicity directions become

$$\hat{\mathbf{h}}_{\ell}^{\pm} = \hat{\mathbf{z}} \pm i\hat{\mathbf{k}}_{\perp} \times \hat{\mathbf{z}},$$

which allows us to write separate equations for u_{ico}^{\pm} and u_{dod}^{\pm} for each scale simply by projecting the corresponding three-dimensional equations to two dimensions. This means that now we need to solve 4×10 equations for each scale or, noting that half of these points are simply reflections of the rest of the points, $4 \times 5 = 20$ equations for each shell.

The fourfold degeneracy which appears upon going from 3D to 2D is remarkable, since in the standard 2D formulation one would consider only vorticity (not helicities of both signs) and only one kind of polygon as a representation of the 2D k space [11]. The effort discussed in this work for going to a 2D formulation may be worthwhile, however, due to the issue of unphysical shell equipartition overwhelming the inverse cascade in 2D logarithmic discretization. A model which has the same topological structure as the 3D one may actually be able to reproduce the $k^{-5/3}$ inverse cascade spectrum without requiring the expensive hierarchical tree approach [24,25]. However, this particular issue is not the focus of the current article, and therefore the concentrated effort necessary for establishing the implications of such a model is left to a future publication.

III. NUMERICAL RESULTS

The model, solves for all three components of the velocity field, with an interaction matrix $M_{n\ell}^{kij}$ representing the Navier-Stokes equation. In order to implement it, an object-oriented approach can be used, where each node has a list of its connecting pairs, as can be inferred from Tables II and III (as shown in Fig. 2), and so that a sum over these pairs can be computed rapidly. The resulting model is a stiff set of ordinary differential equations on an exponentially coarse grid, somewhat similar to the 2D model discussed in Ref. [11].

We have implemented the nested polyhedra model in Python with no parallelization, which is distributed as an open source solver at <http://github.com/gurcani/nestp3d>. It solves $3 \times 8 \times N$ (where N is the number of k -space shells) complex system of equations, for the three components of the velocity field for each half-polyhedra as discussed in Sec. II A. We performed several runs ranging from $N = 30$ to $N = 60$.

The three-dimensional spectra for the highest-resolution case (i.e., $N = 60$) are shown in Fig. 6. As expected, with no

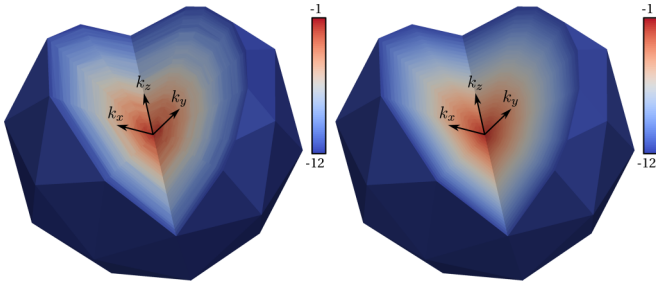


FIG. 6. Resulting instantaneous 3D k spectrum at $t = 250$ (left) and averaged over the range $t = [200, 250]$ (right) for a run with $N = 60$ and $\nu = 10^{-10}$. Here we use a spherical log-log representation, where $E(k_n) = \log_{10}[(u_{n\ell x}^2 + u_{n\ell y}^2 + u_{n\ell z}^2)/k_n]$ is plotted with respect to $\kappa_{n\ell} = \log_{10}(k_n)\hat{\mathbf{k}}_{\ell}$. The resulting spectrum is consistent with the Kolmogorov spectrum $E(k) \propto k^{-5/3}$ as shown in Fig. 7.

source of anisotropy, the resulting spectrum remains perfectly isotropic. Nonetheless, it shows the capability of the model to resolve three-dimensional anisotropy across many decades. The results of the two limiting cases $N = 30$ with $\nu = 10^{-6}$ and $N = 60$ with $\nu = 10^{-10}$ are shown in Fig. 7, where the case $N = 60$ (which takes several weeks to compute on a PC workstation) covers almost six decades in k space and has almost no need for a dissipative range to reach steady state. This seems to be a feature of the model, which may facilitate development of large eddy simulation (LES) versions of itself. As shown in Fig. 7, the truncation from 60 to 30 shells, while varying ν accordingly, has almost no effect on the part of the spectrum that is resolved by the $N = 30$ run. In order to study the effect of the existence of a dissipation range, we have also varied the viscosity coefficient ν . The results for $\nu = 10^{-6}$, $\nu = 2 \times 10^{-7}$, and $\nu = 6 \times 10^{-8}$ are considered for $N = 40$

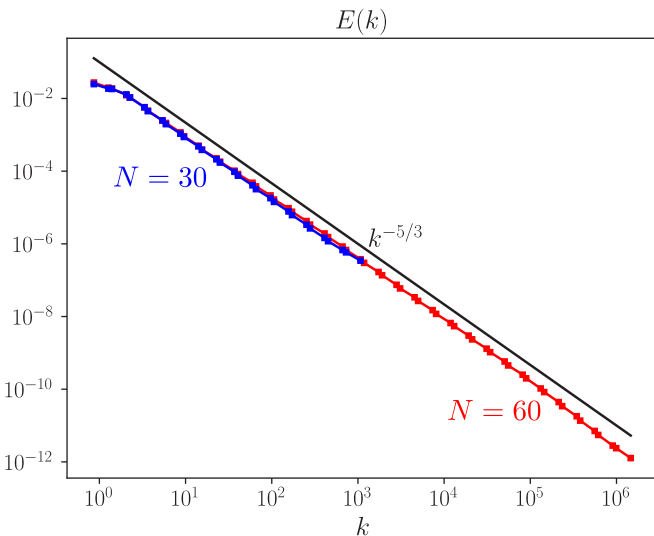


FIG. 7. Log-log plot of the spectral energy density $E(k) = \frac{1}{N_{\ell}k_n} \sum_{\ell,i} |u_{n\ell}^i|^2$ as a function of $k = k_n$. The blue curve that spans from 1 to 10^3 is a run with $N = 30$ and $\nu = 10^{-6}$ averaged in the range $t = [800, 1000]$, whereas the red curve that spans all the way up to 10^6 is a run at the limit of the currently available resolution with $N = 60$ and $\nu = 10^{-10}$ averaged in the range $t = [200, 250]$.

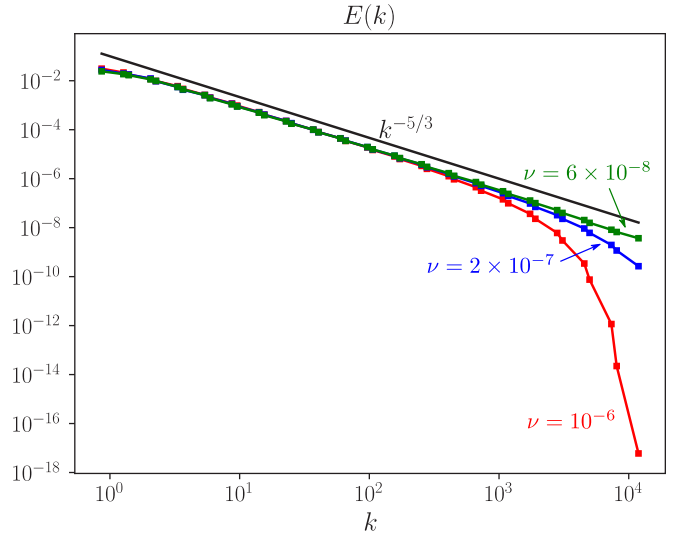


FIG. 8. Log-log plot of the spectral energy density as a function of k (see Fig. 7 for definition) for $N = 40$. The blue curve represents $\nu = 2 \times 10^{-7}$, while the red curve corresponds to $\nu = 10^{-6}$, both averaged in the range $t = [800, 1000]$.

and shown in Fig. 8. As expected, an increasing ν causes a dissipative range to appear, but it does not change either the saturation level or the slope of the spectrum.

Finally, we have performed some preliminary studies of intermittency using this model, and the results are shown in Fig. 9. Curiously, the model shows no sign of intermittency, as it follows the $S_p(k_n) \sim k_n^{-p/3}$ scaling in the inertial range [i.e., $S_p(k_n) = \langle \frac{1}{N_{\ell}} \sum_{\ell} (\sum_i |u_{n\ell}^i|^2)^{p/2} \rangle$ where $\langle \cdot \rangle$ denotes the average over time]. On one hand, this is surprising, since,

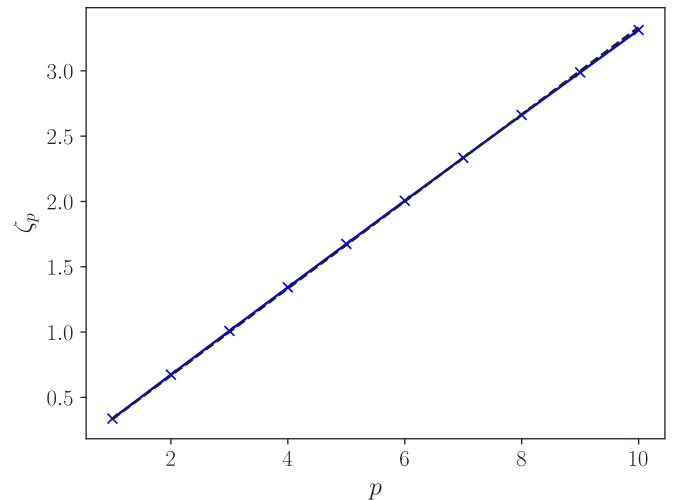


FIG. 9. Index ζ_p of the power law for the structure function of order p [i.e., $S_p(k_n) \sim k_n^{-\zeta_p}$] as a function of p , displaying a clear $S_p(k_n) \sim k_n^{-p/3}$ scaling. The case shown here corresponds to $N = 60$, with $\nu \sim 10^{-10}$, which was averaged only from $t = 200$ to $t = 250$ over shells $N = 4$ to $N = 50$. However, another case with $N = 30$ was integrated up to $t = 25000$ so that an average could be computed from $t = 1000$ to $t = 25000$ over shells 4 to 12, and it gives virtually the same result.

for instance, the GOY model, which can be derived from the nested polyhedra model by additional assumptions about the way the phases are organized, displays dynamical multiscaling and intermittency [21,26], while on the other hand, it is natural, since the model is perfectly self-similar and made of a single three-dimensional “fractal”. In order to further verify that our method of obtaining intermittency is valid, we double-checked our results by repeating the exercise in Ref. [21] with the standard GOY model, as well as a model with alternating shells (i.e., $k_n = k_0 g^n$ for even n and $k_n = k_0 g^n \lambda$ for odd n), and found that while their results are rather robust for shell models, our result of “no intermittency” is similarly robust for our model. We repeated this exercise many times and remain puzzled by these results, since it seems to us paradoxical that the reduction of a reduction can recover a property of the original system that was lost in the first level of reduction. One possible explanation is the fact that shell models do not rely on a single type of triad but are the result of a net transfer of conserved quantity from shell to shell, where many similar triads may play a role. This sense of “net flux” computed over a set of similar triads may be the reason why these models can somehow have intermittent dynamics, while our model, which relies on a single triad family across many scales, does not.

IV. CONCLUSION

The dodecahedron-icosahedron compound discretization of the Navier-Stokes equation proposed in this paper gives the expected wave-number spectrum $k^{-5/3}$ of Kolmogorov and can possibly be used to study the spectra in three-dimensional fluid turbulence. The advantage of a formulation based on logarithmic scaling with a constant number of nodes per scale is that a very large inertial range (i.e., very high Reynolds numbers) can be considered with a much lower number of degrees of freedom. Further simplifications of the model were proposed using the symmetry in k space and the helical decomposition. It was shown that, when isotropy and a particular relation between phases are imposed, the nested polyhedra model reduces to a GOY model. This provides an actual “systematic derivation” of the latter, since the nested polyhedra model itself was obtained by a systematic reduction-decimation of the continuous wave-number space to a finite set of self-similar triads. The straightforward issue of reconstruction of the velocity field from the nested polyhedra description is also discussed in order to demonstrate the richness of the types of flows that the highly reduced model can sustain. Transition to two dimensions is briefly discussed as a reference for future work. It is noteworthy that one can derive a model for describing two-dimensional turbulence which has the same topological network structure as the three-dimensional one. Preliminary studies show that the model described in this paper shows no sign of intermittence since it follows the $S_p(k_n) \sim k_n^{-p/3}$ scaling in the inertial range.

This is curious, since the GOY model, which can be derived from the nested polyhedra model by additional assumptions about the way the phases are organized, displays dynamical multiscaling and intermittency [21,26]. On the other hand, it is natural, since the model is perfectly self-similar and made of a single three-dimensional “fractal”.

Note that the icosahedron and the dodecahedron (i.e., its dual) together form a compound polyhedron called a “dodecahedron-icosahedron compound” (i.e., Wenninger model index 47 [22]). The nested polyhedra model that we introduced here can be seen as a discretization of the k space using these objects. A faceting of this compound polyhedron is a Catalan solid called a “rhombic triacontahedron”, which is also the dual of an Archimedean solid called an “icosidodecahedron”. One could use this connection to “refine” the k space, which is divided into self-similar nested polyhedra, by introducing an icosidodecahedron between two dodecahedron-icosahedron compounds that constitute the nested polyhedra model. The resulting model would use nested “icosidodecahedron–rhombic triacontahedron compounds” as the building blocks for the nested polyhedra model. It would be interesting to determine, using wave-number triad matching conditions, whether more of these complex polyhedra exist, which can be used to develop more and more complex nested polyhedra models. One could then speculate that if one were to initialize the turbulence on an icosahedron in k space, the full system of Navier-Stokes equations (with no truncation) would result in the turbulence energy going from one type of complex polyhedron to another, without ever leaving the space of the compound polyhedra. This is remarkable, as it would transform the infinite system to a set of nested polyhedra. Incidentally, the use of multiple types of polyhedra would also introduce multifractality naturally.

When the approach detailed in this study is applied to a system that supports waves (i.e., linearly), the resulting network model could be suitable for the study of various phenomena including synchronization [27] and small-world or scale freedom [28] since it can be thought of as a complex network of coupled “oscillators” [29]. The structure of the model is somewhat similar to that of models describing food web networks [30] or supply chains, which implies a complex adaptive system. Such analogies are used regularly in plasma turbulence, especially in the presence of large-scale flow structures called zonal flows [31,32]. It would be interesting to see if a similar analogy can be extended to fluid turbulence and to what extent a rigorous mathematical relation can be established between such reduced models of turbulence and analogous ones from biology and other fields.

ACKNOWLEDGMENTS

The author would like to thank P. Morel, P. H. Diamond, R. Grappin and participants, and the organizers of the 8th Festival de Théorie, Aix en Provence.

[1] G. Falkovich, *J. Phys. A* **42**, 123001 (2009).
 [2] U. Frisch, *Turbulence: The Legacy of A. N. Kolmogorov* (Cambridge University Press, Cambridge, UK, 1995).

[3] S. Galtier, S. V. Nazarenko, A. C. Newell, and A. Pouquet, *J. Plasma Phys.* **63**, 447 (2000).
 [4] C. E. Leith, *J. Atmos. Sci.* **28**, 145 (1971).

- [5] J. C. Bowman, *J. Sci. Comput.* **11**, 343 (1996).
- [6] M. Meldi and P. Sagaut, *J. Fluid Mech.* **711**, 364 (2012).
- [7] D. K. Lilly, *J. Atmos. Sci.* **46**, 2026 (1989).
- [8] V. S. L'vov and S. Nazarenko, *JETP Lett.* **83**, 541 (2006).
- [9] I. Thiagalingam and P. Sagaut, *Phys. Fluids* **24**, 115109 (2012).
- [10] L. Biferale, *Annu. Rev. Fluid Mech.* **35**, 441 (2003).
- [11] Ö. D. Gürçan, P. Morel, S. Kobayashi, R. Singh, S. Xu, and P. H. Diamond, *Phys. Rev. E* **94**, 033106 (2016).
- [12] V. Zeitlin, *Physica D: Nonlin. Phenom.* **49**, 353 (1991).
- [13] R. M. Kerr and E. D. Siggia, *J. Stat. Phys.* **19**, 543 (1978).
- [14] J. Eggers and S. Grossmann, *Phys. Fluids A* **3**, 1958 (1991).
- [15] E. Vázquez-Semadeni and J. Scalò, *Phys. Rev. Lett.* **68**, 2921 (1992).
- [16] U. Frisch, P.-L. Sulem, and M. Nelkin, *J. Fluid Mech.* **87**, 719 (1978).
- [17] L. Biferale, A. Lambert, R. Lima, and G. Paladin, *Physica D: Nonlin. Phenom.* **80**, 105 (1995).
- [18] V. S. L'vov, E. Podivilov, A. Pomyalov, I. Procaccia, and D. Vandembroucq, *Phys. Rev. E* **58**, 1811 (1998).
- [19] K. Ohkitani and M. Yamada, *Prog. Theor. Phys.* **81**, 329 (1989).
- [20] M. H. Jensen, G. Paladin, and A. Vulpiani, *Phys. Rev. A* **43**, 798 (1991).
- [21] D. Pisarenko, L. Biferale, D. Courvoisier, U. Frisch, and M. Vergassola, *Phys. Fluids A* **5**, 2533 (1993).
- [22] M. J. Wenninger, *Polyhedron Models* (Cambridge University Press, Cambridge, UK, 1974).
- [23] M. De Pietro, L. Biferale, and A. A. Mailybaev, *Phys. Rev. E* **92**, 043021 (2015).
- [24] E. Aurell, P. Frick, and V. Shaidurov, *Physica D: Nonlin. Phenom.* **72**, 95 (1994).
- [25] E. Aurell, E. Dormy, and P. Frick, *Phys. Rev. E* **56**, 1692 (1997).
- [26] R. Benzi, L. Biferale, R. M. Kerr, and E. Trovatore, *Phys. Rev. E* **53**, 3541 (1996).
- [27] Y. Kuramoto, *Chemical Oscillations, Waves, and Turbulence* (Springer-Verlag, New York, 1984).
- [28] X. F. Wang and G. Chen, *IEEE Circ. Syst. Mag.* **3**, 6 (2003).
- [29] S. H. Strogatz, *Nature* **410**, 268 (2001).
- [30] S. L. Pimm, J. H. Lawton, and J. E. Cohen, *Nature* **350**, 669 (1991).
- [31] P. H. Diamond, S.-I. Itoh, K. Itoh, and T. S. Hahm, *Plasma Phys. Control. Fusion* **47**, R35 (2005).
- [32] Ö. D. Gürçan and P. H. Diamond, *J. Phys. A: Math. Theor.* **48**, 293001 (2015).